Published in final edited form as:
*Biochemistry*. 2011 April 12; 50(14): 3025–3033. doi:10.1021/bi101832w.

# Expression and Biochemical Characterization of the Human Enzyme N-Terminal Asparagine Amidohydrolase (hNTAN1)

**Jason R. Cantor**[1], **Everett M. Stone**[1], and **George Georgiou**[1,2,3,4,*]

[1] Department of Chemical Engineering, University of Texas, Austin, TX 78712

[2] Institute for Cellular and Molecular Biology, University of Texas, Austin, TX 78712

[3] Section of Molecular Genetics and Microbiology, University of Texas, Austin, TX 78712

[4] Department of Biomedical Engineering, University of Texas, Austin, TX 78712

## Abstract

The enzymatic deamidation of N-terminal L-Asn by N-terminal asparagine amidohydrolase (NTAN1) is a feature of the ubiquitin-dependent N-end rule pathway of protein degradation, which relates the *in vivo* half-life of a protein to the identity of its N-terminal residue. Herein we report the bacterial expression, purification, and biochemical characterization of the human NTAN1 (hNTAN1). We show here that hNTAN1 is highly selective for the hydrolysis of N-terminal peptidyl L-Asn, but fails to deamidate free L-Asn or L-Gln, N-terminal peptidyl L-Gln, or acetylated N-terminal peptidyl L-Asn. Similar to other N-terminal deamidases, hNTAN1 is shown to possess a critical Cys residue that is absolutely required for catalysis, corroborated in part by abolishment of activity through the point mutation Cys75Ala. We also present evidence that the exposure of a conserved L-Pro at the N-terminus of hNTAN1 following removal of the initiating L-Met is important for function of the enzyme. The results presented here should assist in the elucidation of molecular mechanisms underlying the neurological defects of NTAN1-deficient mice observed in other studies, and in the discovery of potential physiological substrates targeted by the enzyme in the modulation of protein turnover via the N-end rule pathway.

Targeted proteolytic degradation is essential for the regulation of a variety of cellular processes by achieving the correct balance between protein folding and the degradation of misfolded or damaged proteins (1). In eukaryotes, the ubiquitin (Ub)-proteasome system (UPS) is the primary pathway for the time-specific elimination of targeted proteins and the N-end rule pathway is a subset of this system that relates the *in vivo* half-life of a protein to the identity of its N-terminal residue (2, 3). Degradation signals (degrons) that can be targeted by the N-end rule pathway are of two discrete subsets: N-terminal degrons (N-degrons) and internal degrons (2, 4). The pathway has been observed in all organisms examined, from prokaryotes to eukaryotes, though the former exists in a Ub-independent manner (5). In eukaryotes, an N-degron consists of three determinants: a destabilizing N-terminal residue (Figure 1), one (or more) internal Lys residues (the site of poly-Ub chain

*To whom correspondence should be addressed. Phone: (512)-471-6975 Fax: (512)-471-7963 gg@che.utexas.edu.

Supporting Information Available

Procedures for the purification of recombinant hNTAN1 fused with either a $His_6$ or a strepII affinity tag, a table of the primers used for the work described in this study, and seven figures depicting: the detection of soluble $His_6$-hNTAN1 by Western blot, the purity of hNTAN1-$His_6$ by SDS-PAGE, the purity of hNTAN1-strepII expressed from a plasmid with engineered RBS by SDS-PAGE, the purity of hNTAN1-FLAG-strepII expressed from pNTAN2FLAGSII by SDS-PAGE, an HPLC trace overlay of $N^1$-AII, AII, and hNTAN1-mediated deamidation of $N^1$-AII, the Michaelis-Menten curves generated for determination of hNTAN1 kinetic parameters, and an alignment of multiple vertebrate NTAN1 sequences revealing a conserved Pro2, This material is available free of charge via the Internet at http://pubs.acs.org.

formation), and a conformationally flexible region in the vicinity of this internal Lys (6, 7). An N-degron can be generated from a precursor, called a pre-N-degron, through specific protease-mediated post-translational modifications (8).

The N-end rule has a hierarchical structure (Figure 1). In eukaryotes, N-terminal L-Asn and L-Gln function as tertiary destabilizing residues through their deamidation by N-terminal amidohydrolases (Nt-amidases) into the secondary destabilizing N-terminal residues L-Asp and L-Glu, respectively (9–11). The secondary destabilizing activity of N-terminal L-Asp and L-Glu requires their conjugation to L-Arg by the *ATE1*-encoded Arg-tRNA protein transferase (R-transferase) (12–14). In mammals and other eukaryotes that produce nitric oxide (NO), N-terminal L-Cys can also function as a tertiary destabilizing residue through its oxidation to Cys-sulfinate or Cys-sulfonate in an $O_2$- or NO-dependent manner, whereby the oxidized L-Cys can be arginylated by ATE1 (8, 13). Together with other primary destabilizing residues, the N-terminal L-Arg allows for protein substrate recognition by specific E3 Ub ligases and subsequent degradation (15).

A number of genetic studies with knock-out mice have implicated involvement of the N-end rule pathway in cardiac development and signaling, angiogenesis (12, 16), meiosis (17), DNA repair (18), neurogenesis (16), pancreatic functions (19), learning and memory (10, 20), female development (17), muscle atrophy (21), and olfaction (22). Other functions of the pathway include: (i) selective degradation of misfolded proteins (23), (ii) sensing of nitric oxide, oxygen, and heme (12–14, 24), (iii) regulation of short peptide import (25, 26), (iv) fidelity of chromosome segregation (27), (v) regulation of apoptosis through NTAN-1 mediated degradation of the caspase-mediated C-terminal fragment of *Drosophila* inhibitor of apoptosis 1 (DIAP1) (28), and (vi) regulation of leaf senescence in plants (29).

In contrast to *S. cerevisiae* which possesses a single enzyme (Nta1) that can deamidate either L-Asn or L-Gln at the N-terminus of a protein substrate (9), vertebrates possess one distinct enzyme for the specific deamidation of N-terminal L-Asn (NTAN1) and one for the specific deamidation of N-terminal L-Gln (NTAQ1) (11). NTAN1-deficient mice were found to display neurological defects such as impairment of spontaneous activity, spatial memory, and in socially conditioned exploratory behavior (10).

In an earlier study, an enzyme with N-terminal L-Asn hydrolase activity from porcine liver was purified and partially characterized (30). A gene encoding a putative NTAN1 enzyme, *Ntan1*, was subsequently isolated from a mouse cDNA library and shown to complement a *S. cerevisiae* Δ*nta1* mutant strain (31). Herein, we describe the expression and biochemical characterization of the human NTAN1 (hNTAN1). Among our results, we have identified an essential L-Cys residue that is critical for the hydrolysis of N-terminal L-Asn by hNTAN1, and thus may act as a nucleophile in catalysis, in analogy with both the *S. cerevisiae* Nta1 (9) and the dedicated murine N-terminal L-Gln deamidase NTAQ1 (11).

## EXPERIMENTAL PROCEDURES

### Materials

Synthetic oligonucleotides were purchased from Integrated DNA Technologies (Coralvillle, IA). Restriction enodnucleases, *Vent* DNA polymerase, T4 DNA ligase, and dNTPs were from New England Biolabs (Ipswich, MA). Nickel-nitrilotriacetic acid ($Ni^{2+}$-NTA) resin was from QIAGEN (Valencia, CA). Strep-Tactin Superflow high capacity suspension and D-Desthiobiotin were obtained from IBA GmbH (St. Louis, MO). Anti-FLAG M2 magnetic beads, FLAG peptide, $Val^5$-angiotensin II (AII), and $Asn^1Val^5$-angiotensin II ($N^1$-AII) were purchased from Sigma-Aldrich (St. Louis, MO). $Gln^1Val^5$-angiotensin II ($Q^1$-AII), Ac-$Asn^1Val^5$-angiontensinII (Ac-$N^1$-AII), and a 9mer peptide ($N^1$-DIAP) corresponding to the

N-terminus of the caspase-mediated C-terminal fragment of DIAP1 (28) were purchased from Abgent Inc. (San Diego, CA). Difco 2xYT growth medium was from Becton Dickinson (Franklin Lakes, NJ). All other reagents were obtained from Sigma-Aldrich (St. Louis, MO) unless otherwise noted.

## Construction of hNTAN Expression Plasmids

A gene encoding the human protein N-terminal asparagine amidohydrolase (hNTAN1) (933bp) with a fused N-terminal $His_6$ affinity tag was synthetically assembled using a set of codon-optimized overlapping oligonucleotides designed by the program DNAWorks as described previously (32). *NcoI* and *EcoRI* restriction sites were incorporated into the outermost sense and antisense oligonucleotides respectively. Sense primers (Table S1 of the Supporting Information) were designed to: (i) introduce the hNTAN1 initiation codon within an *NcoI* site thereby eliminating the N-terminal $His_6$ affinity tag (NTAN-N-NoHis) and (ii) modify the ribosome binding site (RBS) and incorporate an upstream *XbaI* site in order to improve the translation initiation rate of hNTAN1 in *E. coli* (NTAN-RBS2). Antisense primers were designed to append a C-terminal $His_6$ affinity tag (NTAN-C-H), a C-terminal strepII affinity tag (NTAN-C-SII), and a C-terminal FLAG-strepII tandem affinity tag (NTAN-C-FSII), all followed by a *NotI* site. Lastly, a sense primer (NTAN-MP-RBS2) was designed to eliminate the GGA codon immediately following the initiation ATG (within an *NcoI* site) that was incorporated to maintain a correct open reading frame in the cassettes described above. Individual PCR products for each cassette were digested accordingly and ligated into pET28-a (Novagen). The RBS and the N- and C-terminal amino acid sequences of each hNTAN1 construct created are listed in Table 1. *E. coli* BL21 (DE3) was used for protein expression and purification. Genes encoding hNTAN1 mutants C75A, C75S, C75T, or C160A, were constructed by overlap-extension PCR using the pNTAN2FLAGSII plasmid as template and the primer pairs shown in Table S1 of the Supporting Information.

## Expression and purification of recombinant hNTAN1

*E. coli* BL21(DE3) cells transformed with pNTAN2FLAGSII were cultured overnight at 37°C in 2xYT medium supplemented with 30μg/mL kanamycin and used to inoculate 500mL fresh medium (1:100 dilution). When the absorbance at 600nm ($A_{600}$) reached 0.5–0.7, the cells were transferred to 25°C and allowed to equilibrate for 20 min, at which point the culture was supplemented with IPTG to a final concentration of 1mM to induce protein expression. After 16 hr incubation at 25°C, the cells were harvested by centrifugation at 10,000× *g* for 10 min. hNTAN1 was subsequently purified by tandem strepII affinity chromatography and immobilized anti-FLAG as follows: cell pellets were resuspended in 15mL buffer W (100mM Tris-HCl, 150mM NaCl, 1mM EDTA, pH 8) on ice, and then lysed by three passes through a French pressure cell. Debris was removed by centrifugation at 40,000× *g* for 45 min and the resulting supernatant (soluble fraction) was decanted and applied to a 5mL polypropylene column (Pierce) packed with 300$\mu$L of strep-tactic superflow high capacity resin (33). The column flow-through was collected and re-applied to the column for 3 total passes. The resin was then washed with 30 bed volumes buffer W and 10 bed volumes buffer W2 (buffer W containing 100$\mu$M D-Desthiobiotin) before the resin was incubated with 10 bed volumes buffer E (buffer W containing 2.5mM D-Desthiobiotin) and the eluant was collected. All purification steps were performed at 4°C. The elution fraction was applied to an Amicon Ultra 10K MWCO filter, concentrated to a final volume of 1mL in buffer W, and then incubated with 200$\mu$L anti-FLAG M2 magnetic beads for 1 hr at room temperature with gentle rotation. The magnetic beads were then collected using a magnetic separator (Dynal MPC-S, Invitrogen) to remove the supernatant, and washed with 30 bed volumes buffer W before the purified protein was collected by competitive elution with 5 bed volumes of buffer W containing 100$\mu$g/mL FLAG peptide by gentle rotation for 10 min at room temperature. The final eluant was applied to an Amicon

Ultra 10K MWCO filter, concentrated to a final volume of 100$\mu$L in storage buffer (50mM Tris-HCl, 150mM NaCl, 1mM EDTA, 0.5mM dTT pH 7.5) and stored at 4°C. Procedures for the purification of recombinant hNTAN1 fused to either a $His_6$ or a strepII affinity tag can be found in the Supporting Information. Protein concentrations were determined using a calculated extinction coefficient of 32,430 $M^{-1}cm^{-1}$ (34).

### Activity assays

For kinetic analyses, hNTAN1 (40–50nM purified enzyme) was incubated with substrate (concentrations from 0–5 × $K_M$) at 37°C in assay buffer (50mM Tris-HCl, 150mM NaCl, pH 7.5) at a total volume of 100$\mu$L, and at desired times reactions were quenched with 5$\mu$L of 12% (w/v) trichloroacetic acid (TCA). Product formation was determined by HPLC as follows: For the substrate $Asn^1Val^5$-angiotensin II ($N^1$-AII), an aliquot of the quenched reaction was brought to a final volume of 100$\mu$L with assay buffer and then injected into a Phenomenex C18 reverse-phase column followed by elution with: 5% ACN, 95% $H_2O$ for 2 min, increasing to 21% ACN, 79% $H_2O$ over 3 min, then increasing to 24.7% ACN, 75.3% $H_2O$ over 11 min, and finally increasing to 95% ACN, 5% $H_2O$ over 3 min before returning to 5% ACN, 95% $H_2O$ over 3 min. Both solvents contained 0.1% trifluoroacetic acid (TFA). The product concentration was determined using the integration area at 280nm and a standard curve generated under the same conditions with $Val^5$-angiotensin II (AII). For the substrates L-Asn and L-Gln, following quenching, reaction products were derivatized with *o*-phthalaldehyde (OPA) and analyzed by HPLC as described previously (32). A description of the HPLC program employed to evaluate activity for the substrate $N^1$-DIAP can be found in the Supporting Information. All reactions were done at least in triplicate and the observed rates were fit to the Michaelis-Menten equation using Kaleidagraph (Synergy).

The effect of pH on hNTAN1 activity was determined in 50mM Bis-Tris, pH 6.0–6.5, 50mM Tris-HCl, pH 7.0–8.5, or 50mM CAPSO, pH 10, and 150mM NaCl. Enzyme was preincubated in buffer and reactions were initiated by the addition of preincubated enzyme (1nM) to 25$\mu$M $N^1$-AII at 37°C in the appropriate pH buffer. After 1.5 min, reactions were quenched and analyzed by HPLC as described earlier.

The effects of various divalent salts, EDTA and D-desthiobiotin on hNTAN1 activity were determined by preincubating enzyme (20nM) in assay buffer at 4°C for 3 hr with either EDTA (1mM), D-desthiobiotin (3mM), or a divalent salt (1mM). Reactions were initiated by the addition of the preincubated enzyme (1nM) to 100$\mu$M $N^1$-AII in assay buffer at 37°C. After 4 min, the reactions were quenched and analyzed by HPLC as described earlier.

### Circular Dichroism (CD)

Far-UV CD spectra were measured at 200–260nm using a J-815 CD spectrometer (Jasco, Easton, MD) equipped with a temperature-controlled cell holder set to room temperature, using 15$\mu$M enzyme in 50mM Tris-HCl, 150mM NaCl, 1mM EDTA, 0.5mM dTT, pH 7.5. CD thermal melting curves were generated by obtaining the CD spectra at 210nm from 20–80°C at a rate of 1°C/min in 50mM Tris-HCl, 150mM NaCl, 1mM EDTA, 0.5mM dTT, pH 7.5. Data points were collected at 5°C intervals and $T_M$ values were subsequently determined as the inflection point of sigmoidal curves fit to each data set using Kaliedagraph.

## RESULTS

### Construction of a synthetic hNTAN1 gene

The human NTAN1 gene (GenBank accession no: NM_173474) contains a number of rare *E. coli* codons, including 13 such Arg codons (AGA, AGG, and CGA). The presence of rare

codons has been shown to be detrimental to the expression of several recombinant proteins (35). A synthetic hNTAN1 gene fused to a 5′ sequence encoding a $His_6$ affinity tag was constructed and expressed in *E. coli* BL21 (DE3). Western blot analysis with an anti-His tag antibody as described previously (36) revealed the presence of a band with the expected M.W. (~35kDa) in both the soluble and insoluble fractions (Figure S1 of the Supporting Information). However, the purified $His_6$-hNTAN1 enzyme was found to be minimally active towards the substrate $N^1$-AII (Table 1). In contrast, fusion of a $His_6$ affinity tag at the C-terminus of hNTAN1 led to the expression of enzyme (Figure S2 of the Supporting Information) with much higher specific activity towards $N^1$-$A^{II}$, indicating that an unoccluded N-terminus may be important for catalysis. In subsequent studies, it was found that hNTAN1 activity was inhibited by $Ni^{2+}$ or $Co^{2+}$ and therefore, for purification purposes, the C-terminal $His_6$ tag was replaced with a strepII peptide affinity tag (pR1NTANSII) and accordingly, EDTA was included in all purification buffers.

To improve the expression yield, the RBS calculator (37) was used to design an optimized ribosomal binding site for more efficient translation initiation. Upon expression of hNTAN1-strepII using the engineered RBS sequence from plasmid pR2NTANSII, the expression yield of hNTAN1 increased 2–3-fold, while protein purity following strepII affinity chromatography concomitantly increased from 30% to approximately 70% (Table 1) as determined by SDS-PAGE (Figure S3 of the Supporting Information). To further improve the purity of hNTAN1 following affinity chromatography, we constructed a plasmid encoding a tandem C-terminal FLAG-strepII affinity tag (pNTANFLAGSII). With this construct, the eluant obtained from the strepII affinity chromatography step was loaded onto magnetic beads with an immobilized anti-FLAG monoclonal antibody, and eluted with buffer containing a large excess of synthetic FLAG. Using this tandem affinity chromatography procedure, we obtained ~0.2mg/L recombinant hNTAN1 that was determined to be > 98% homogeneous by SDS-PAGE (Figure 2).

ESI-MS analysis of the purified hNTAN1 revealed the presence of two major peaks of 37,208 ± 12 and 37,020 ± 12 *m/z* at a ~3:1 intensity ratio (Figure 3A). The M.W. of the latter peak was in agreement with the predicted M.W. of the enzyme (37,026 Da). The 37,208 ± 12 peak was consistent with an hNTAN1 species containing the initiating L-Met and an L-Gly at position 2 that was introduced during cloning (37,214 Da). Although the *E. coli* methionine aminopeptidase (MAP) is highly efficient in removing the initiating L-Met residue when L-Gly occupies P1′ of a protein substrate, its catalytic efficiency is severely compromised when the P2′ residue is L-Pro (38), as was the case in the hNTAN1 enzyme expressed from plasmid pNTANFLAGSII. To prevent the accumulation of unprocessed L-Met-L-Gly-hNTAN1, we generated a modified construct (pNTAN2FLAGSII) in which the L-Gly at +2 was eliminated. MS analysis of the purified protein obtained from cells transformed with the pNTAN2FLAGSII revealed a single peak of the expected M.W. for hNTAN1 in which the initiating L-Met had been removed by MAP (*m/z* of 37,022 ± 12) (Figure 3B). It is worth noting that *E. coli* MAP is highly efficient in removing the initiating L-Met residue when L-Pro occupies P1′ and L-Leu occupies P2′ (38) given that native hNTAN1 contains L-Pro at +2 and L-Leu at +3.

## Biochemical characterization of hNTAN1

The kinetics for hydrolysis of N-terminal L-Asn angiontensin ($N^1$-$A^{II}$) by hNTAN1 (Table 2) purified from either pNTANFLAGSII or pNTAN2FLAGSII (Table 1) were determined by HPLC (Figure S5). In both cases, the data could be fit to a Michaelis-Menten model (Figure S6). hNTAN1 exhibited nearly identical $K_M$ values ($K_M = 31\mu M$; pNTANFLAGSII and $K_M = 35\mu M$; pNTAN2FLAGSII) independent of the expression construct; however, hNTAN1 expressed from pNTAN2FLAGSII in which the L-Gly at +2 was eliminated, displayed a nearly 3-fold greater $k_{cat}$ ($k_{cat} = 2.3s^{-1}$; pNTANFLAGSII and $k_{cat} = 6.6s^{-1}$;

pNTAN2GLAGSII). This result indicates that the presence of the conserved L-Pro residue (Figure S7 of the Supporting Information) at the N-terminus of hNTAN1 is important for catalysis and is corroborated by the ESI-MS analysis described above.

hNTAN1 was unable to hydrolyze $Q^1$-AII, Ac-$N^1$-AII, L-Asn, and L-Gln, indicating that the recombinant human enzyme displayed a substrate specificity analogous to that of the isoform previously purified from porcine liver (30). Moreover, hNTAN1 was unable to hydrolyze $N^1$-DIAP (data not shown), suggesting the possibility that NTAN1-mediated deamidation of the DIAP1 substrate *in vivo* (28) may be additionally dependent on interactions between NTAN1 and other (unidentified) protein factors.

The effect of pH on hNTAN1 activity with $N^1$-AII is shown in Figure 4, which revealed that the enzyme exhibited an activity optimum between pH 6.0–7.5, followed by a sharp decline in activity at alkaline pH. Our approximation for pH dependence of hNTAN1 activity suggests that the protonation of a single group within the enzyme is crucial for catalysis, resulting in a pH-dependence curve with a single descending limb p*K*a of 8.2 ± 0.06.

As summarized in Table 3, low micromolar concentrations of $Zn^{2+}$ and $Cu^{2+}$ completely inhibit hNTAN1 activity, while 50$\mu$M $Ni^{2+}$, $Co^{2+}$, or $Mn^{2+}$ only partially inhibited the hydrolysis of $N^1$-AII. Further, $Mg^{2+}$, $Ca^{2+}$, EDTA, and D-desthiobiotin did not impart any noticeable effects on the activity of hNTAN1.

### Phylogenetic conservation and mutagenesis of conserved Cys residues in hNTAN1

Given prior validation that the functionally similar enzymes *S. cerevisiase* Nta1 (9) and murine NTAQ1 (11) each possess an essential catalytic cysteine residue, we explored the possibility that hNTAN1 contained an analogous activity-dependent cysteine residue. A Position Specific Iterative BLAST (PSI-BLAST) (39) search was carried out with the complete amino acid sequence of hNTAN1 to determine the phylogenetic conservation across each of the enzyme's five cysteines, as those residues exhibiting the highest degree of conservation would be implicated as having a higher likelihood for functional and/or structural essentiality. Sequence alignment of hNTAN1 with the PSI-BLAST results (n = 106) revealed two distinct cysteine conservation groupings: (i) C75 and C160 (70% and 66% Cys frequencies respectively), and (ii) C89, C93, and C118 (28%, 22%, and 13% Cys frequencies respectively) (Figure 5). The C75 and C160 in hNTAN1 were substituted with L-Ala and the relative hydrolysis of $N^1$-AII by the respective protein mutants was determined (Table 4). While replacement of C160 with L-Ala had no effect on the catalytic activity, the C75A variant enzyme was completely inactive. This finding indicates that C75 is essential for enzymatic activity and likely to constitute the catalytic nucleophile. The substitution of C75 with other nucleophilic amino acids, namely L-Ser or L-Thr, failed to restore activity.

Analysis of the CD spectrum of recombinant hNTAN1 indicated 30% helical, 20% sheet, 20% turn, and 30% random structure (Table 5). The mutation C75A resulted in no obvious change in CD spectra or secondary structure composition (Figure 6), further supporting the suggestion that the inactivity of this variant was strictly due to the removal of the potentially nucleophilic thiol group and not to changes in folding.

## DISCUSSION

A number of biochemical and genetic studies over the past twenty years have begun to elucidate the significance of the N-end rule pathway in numerous physiological processes and have revealed many of the critical components involved in this subset of the UPS-dependent proteolytic quality control system. Proteolysis by the N-end rule pathway is

dependent upon distinct types of degradation signals (degrons). In vertebrates, N-terminal L-Asn and L-Gln can function as tertiary destabilizing residues of the N-end rule pathway through enzymatic deamidation by either NTAN1 (Asn-specific) or NTAQ1 (Gln-specific) to yield the secondary destabilizing N-terminal L-Asp and L-Glu, respectively.

Almost 20 years ago, a mammalian monomeric enzyme purified from the cytosolic fraction of porcine liver cells (30) was shown to exhibit L-Asn-specific Nt amidase activity. More recently, a murine cDNA that complemented a S. cerevisiase Δnta1 mutant was identified, though the protein was not characterized enzymologically (31). Interestingly, the murine gene that was able to complement the S. cerevisiase Δnta1 mutant displays only 10% amino acid sequence identity to the recently described murine L--Gln-specific Nt amidase, NTAQ1 (11), and only 12% amino acid sequence identity to the S. cerevisiase Nta1 (9), which deamidates both L-Asn and L-Gln at the N-terminus of a protein substrate.

Because of its high degree of sequence homology to other mammalian NTAN1s (e.g. murine and porcine) a putative NTAN1 gene from *Homo sapiens* (hNTAN1) has been assigned, though direct experimental evidence of its activity and biochemical characterization had been lacking. Here, we report that bacterial expression and kinetic characterization of hNTAN1. Expression of hNTAN1 in *E. coli* at preparative levels was achieved through the use of a codon optimized gene and an optimal RBS and translation initiation region for efficient protein synthesis. Two lines of evidence suggested that the N-terminus of hNTAN1 is important for its enzymatic activity. First, enzyme expressed with an N-terminal epitope tag exhibited substantially lower activity relative to enzyme expressed with a C-terminal epitope tag, as evaluated by deamidation of $N^1$-AII (Table 1). Second, the presence of an N-terminal L-Met-L-Gly dipeptide, which partially interfered with processing by the *E. coli* methionine aminopeptidase (MAP), resulted in an enzyme preparation containing an approximately 3:1 ratio of L-Met-L-Gly-hNTAN1 to MAP-processed hNTAN1 with an exposed L-Pro at the N-terminus. This mixed preparation had nearly 3-fold lower specific activity relative to a preparation of the authentic human enzyme. Thus, we concluded that the exposure of the conserved L-Pro residue at the N-terminus is important for the function of the enzyme.

Kinetic analysis revealed that hNTAN1 is highly selective for the hydrolysis of N-terminal peptidyl L-Asn, but fails to deamidate free L-Asn or L-Gln, N-terminal peptidyl L-Gln (in $Q^I$-AII), or acetylated N-terminal peptidyl L-Asn (in Ac-$N^1$-AII). The human enzyme displayed approximately 10-fold lower $K_M$ and 100-fold lower $k_{cat}$ for the $N^1$-AII peptide relative to the results reported by Stewart et al. (30) for the porcine enzyme under similar assay conditions. However, we note that the total yield of the purified porcine enzyme reported in that study was less than 2$\mu$g, raising the possibility that inaccuracies in the quantification of very small amounts of protein used in that study may have led to an overestimation of the $k_{cat}$ value. Nonetheless, it is also possible that the difference in catalytic activity may be due to the slight differences in the primary sequence between the human and porcine NTAN1 isoforms (92% amino acid sequence identity), or perhaps because the recombinant human enzyme may be lacking a factor present in liver tissue.

The recombinant hNTAN1 displayed a pH optimum in the range 6.0–7.5, with a sharp decline in activity upon shifting to more alkaline pH, indicating that protonation of a single group is important for catalysis. The pH dependence of hNTAN1 and its sensitivity to the alkylating agent iodoacetamide suggest that a reactive thiolate may have an important role in catalysis. PSI-BLAST blast analysis of hNTAN1 homologues revealed two highly conserved L-Cys residues. Site-specific mutagenesis subsequently demonstrated that the substitution of C75 with L-Ala completely abolishes activity, but does not affect the secondary structure of the enzyme as determined by circular dichroic spectra. Further,

neither L-Ser nor L-Thr could replace C75 and concomitantly maintain enzyme function, revealing that this residue is absolutely required for catalysis. Therefore, similar to both the yeast Nta1 and the recently reported NTAQ1, the human NTAN1 appears to possess a critical nucleophilic L-Cys.

Although NTAN1 has been implicated in the modulation of protein turnover via the N-end rule pathway, very little is known with respect to: (i) the exact molecular mechanisms or interactive processes underlying the neurological defects observed in *Ntan1*$^{-/-}$ mice (10), (ii) the catalytic mechanism and nature of the active site structure of NTAN1, which shares little sequence similarity to other amidases, and (iii) the identity of actual physiological substrates targeted by the enzyme.

While it is conceivable to scan the proteome for amino-terminal sequences of the type L-Met-L-Asn (or L-Met-L-Gln), the prediction of physiological substrates targeted by NTAN1 (or NTAQ1) is inherently complicated due to the potentially vast contribution of endoproteolysis in generating N-terminal degrons of these types. This point was illustrated by the discovery of NTAN1-mediated degradation of DIAP1 in the regulation of apoptosis (28). DIAP1 is cleaved by a caspase to generate a C-terminal fragment with N-terminal L-Asn, which is then targeted through the NTAN1-ATE1 pathway in ultimately generating a primary destabilizing N-terminal L-Arg for subsequent substrate protein degradation. To date, DIAP1 remains the only known substrate of N-terminal L-Asn deamidation. However, we describe here that hNTAN1 was unable to deamidate the N-terminal L-Asn of a synthetic 9mer corresponding to the N-terminus of the caspase-mediated C-terminal fragment (in $N^1$-DIAP), suggesting the possibility that NTAN1-mediated deamidation of the DIAP1 substrate *in vivo* may be dependent on additional interactions between the enzyme and other (unidentified) protein factors.

The enzymological characterization of N-end rule pathway components such as hNTAN1 should assist in the elucidation of their physiological roles, allow for the *in vitro* reconstruction of the pathway itself, and subsequently, aid in the discovery of potential physiological substrates targeted by its components. Further, recombinant expression of the human homologues of these components could present an opportunity to specifically investigate mechanisms and features of human pathological states associated with protein misfolding and aggregation, some of which may be associated with the N-end rule pathway.

## Supplementary Material

Refer to Web version on PubMed Central for supplementary material.

## Acknowledgments

This work was supported by grants from National Institutes of Health Grant CA139059 and the Cancer Prevention and Research Initiative of Texas (CPRIT). J.R.C. also acknowledges the U.S. Department of Homeland Security (DHS) for a Graduate Fellowship under the DHS Scholarship and Fellowship Program.

The authors thank Stony Lo for generating ESI-MS mass spectra, and thank Eun Jeong Cho for assistance with obtaining CD spectra.

## Abbreviations

| | |
|---|---|
| **Ac-$N^1$-AII** | N-acetyl-Asn$^1$Val$^5$-angiotensin II (Ac-NRVYVHPF) |
| **ACN** | acetonitrile |
| **ATE1** | arginyltransferase 1 |

| | |
|---|---|
| **AII** | $Val^5$-angtiotensin II (DRVYVHPF) |
| **CD** | circular dichroism |
| **DIAP1** | *Drosophila* inhibitor of apoptosis 1 |
| **ESI-MS** | electrospray ionization-mass spectrometry |
| **IPTG** | isopropyl β-D-1-thiogalactopyranoside |
| **MAP** | methionine aminopeptidase |
| **$N^1$-AII** | $Asn^1Val^5$-angiotensin II (NRVYVHPF) |
| **$N^1$-DIAP** | 9mer corresponding to the N-terminus of the caspase-mediated C-terminal fragment of DIAP1 (NNTNATQLF) |
| **Nta1** | N-terminal amidase 1 |
| **Nt-amidase** | N-terminal amidohydrolase |
| **NTAN1** | N-terminal asparagine amidohydrolase |
| **NTAQ1** | N-terminal glutamine amidohydrolase |
| **PSI-BLAST** | Position-specific iterative BLAST |
| **$Q^1$-AII** | $Gln^1Val^5$-angiotensin II (QRVYVHPF) |
| **Ub** | ubiquitin |
| **UPS** | ubiquitin-proteasome system |

## References


1. McClellan AJ, Tam S, Kaganovich D, Frydman J. Protein quality control: chaperones culling corrupt conformations. Nat Cell Biol. 2005; 7:736–741. [PubMed: 16056264]
2. Varshavsky A. The N-end rule: functions, mysteries, uses. Proc Natl Acad Sci U S A. 1996; 93:12142–12149. [PubMed: 8901547]
3. Mogk A, Schmidt R, Bukau B. The N-end rule pathway for regulated proteolysis: prokaryotic and eukaryotic strategies. Trends Cell Biol. 2007; 17:165–172. [PubMed: 17306546]
4. Ravid T, Hochstrasser M. Diversity of degradation signals in the ubiquitin-proteasome system. Nat Rev Mol Cell Biol. 2008; 9:679–690. [PubMed: 18698327]
5. Varshavsky A. The N-end rule pathway of protein degradation. Genes Cells. 1997; 2:13–28. [PubMed: 9112437]
6. Bachmair A, Varshavsky A. The degradation signal in a short-lived protein. Cell. 1989; 56:1019–1032. [PubMed: 2538246]
7. Prakash S, Inobe T, Hatch AJ, Matouschek A. Substrate selection by the proteasome during degradation of protein complexes. Nat Chem Biol. 2009; 5:29–36. [PubMed: 19029916]
8. Tasaki T, Kwon YT. The mammalian N-end rule pathway: new insights into its components and physiological roles. Trends Biochem Sci. 2007; 32:520–528. [PubMed: 17962019]
9. Baker RT, Varshavsky A. Yeast N-terminal amidase. A new enzyme and component of the N-end rule pathway. J Biol Chem. 1995; 270:12065–12074. [PubMed: 7744855]
10. Kwon YT, Balogh SA, Davydov IV, Kashina AS, Yoon JK, Xie Y, Gaur A, Hyde L, Denenberg VH, Varshavsky A. Altered activity, social behavior, and spatial memory in mice lacking the NTAN1p amidase and the asparagine branch of the N-end rule pathway. Mol Cell Biol. 2000; 20:4135–4148. [PubMed: 10805755]
11. Wang H, Piatkov KI, Brower CS, Varshavsky A. Glutamine-specific N-terminal amidase, a component of the N-end rule pathway. Molecular Cell. 2009; 34:686–695. [PubMed: 19560421]

12. Kwon YT, Kashina AS, Davydov IV, Hu RG, An JY, Seo JW, Du F, Varshavsky A. An essential role of N-terminal arginylation in cardiovascular development. Science. 2002; 297:96–99. [PubMed: 12098698]
13. Hu RG, Sheng J, Qi X, Xu Z, Takahashi TT, Varshavsky A. The N-end rule pathway as a nitric oxide sensor controlling the levels of multiple regulators. Nature. 2005; 437:981–986. [PubMed: 16222293]
14. Hu RG, Wang H, Xia Z, Varshavsky A. The N-end rule pathway is a sensor of heme. Proc Natl Acad Sci U S A. 2008; 105:76–81. [PubMed: 18162538]
15. Kwon YT, Reiss Y, Fried VA, Hershko A, Yoon JK, Gonda DK, Sangan P, Copeland NG, Jenkins NA, Varshavsky A. The mouse and human genes encoding the recognition component of the N-end rule pathway. Proc Natl Acad Sci U S A. 1998; 95:7898–7903. [PubMed: 9653112]
16. An JY, Seo JW, Tasaki T, Lee MJ, Varshavsky A, Kwon YT. Impaired neurogenesis and cardiovascular development in mice lacking the E3 ubiquitin ligases UBR1 and UBR2 of the N-end rule pathway. Proc Natl Acad Sci U S A. 2006; 103:6212–6217. [PubMed: 16606826]
17. Kwon YT, Xia Z, An JY, Tasaki T, Davydov IV, Seo JW, Sheng J, Xie Y, Varshavsky A. Female lethality and apoptosis of spermatocytes in mice lacking the UBR2 ubiquitin ligase of the N-end rule pathway. Mol Cell Biol. 2003; 23:8255–8271. [PubMed: 14585983]
18. Ouyang Y, Kwon YT, An JY, Eller D, Tsai SC, Diaz-Perez S, Troke JJ, Teitell MA, Marahrens Y. Loss of Ubr2, an E3 ubiquitin ligase, leads to chromosome fragility and impaired homologous recombinational repair. Mutat Res. 2006; 596:64–75. [PubMed: 16488448]
19. Zenker M, Mayerle J, Lerch MM, Tagariello A, Zerres K, Durie PR, Beier M, Hulskamp G, Guzman C, Rehder H, Beemer FA, Hamel B, Vanlieferinghen P, Gershoni-Baruch R, Vieira MW, Dumic M, Auslender R, Gil-da-Silva-Lopes VL, Steinlicht S, Rauh M, Shalev SA, Thiel C, Ekici AB, Winterpacht A, Kwon YT, Varshavsky A, Reis A. Deficiency of UBR1, a ubiquitin ligase of the N-end rule pathway, causes pancreatic dysfunction, malformations and mental retardation (Johanson-Blizzard syndrome). Nat Genet. 2005; 37:1345–1350. [PubMed: 16311597]
20. Balogh SA, Kwon YT, Denenberg VH. Varying intertrial interval reveals temporally defined memory deficits and enhancements in NTAN1-deficient mice. Learn Mem. 2000; 7:279–286. [PubMed: 11040259]
21. Lecker SH, Solomon V, Price SR, Kwon YT, Mitch WE, Goldberg AL. Ubiquitin conjugation by the N-end rule pathway and mRNAs for its components increase in muscles of diabetic rats. J Clin Invest. 1999; 104:1411–1420. [PubMed: 10562303]
22. Tasaki T, Sohr R, Xia Z, Hellweg R, Hortnagl H, Varshavsky A, Kwon YT. Biochemical and genetic studies of UBR3, a ubiquitin ligase with a function in olfactory and other sensory systems. J Biol Chem. 2007; 282:18510–18520. [PubMed: 17462990]
23. Eisele F, Wolf DH. Degradation of misfolded protein in the cytoplasm is mediated by the ubiquitin ligase Ubr1. FEBS Lett. 2008; 582:4143–4146. [PubMed: 19041308]
24. Lee MJ, Tasaki T, Moroi K, An JY, Kimura S, Davydov IV, Kwon YT. RGS4 and RGS5 are in vivo substrates of the N-end rule pathway. Proc Natl Acad Sci U S A. 2005; 102:15030–15035. [PubMed: 16217033]
25. Du F, Navarro-Garcia F, Xia Z, Tasaki T, Varshavsky A. Pairs of dipeptides synergistically activate the binding of substrate by ubiquitin ligase through dissociation of its autoinhibitory domain. Proc Natl Acad Sci U S A. 2002; 99:14110–14115. [PubMed: 12391316]
26. Turner GC, Du F, Varshavsky A. Peptides accelerate their uptake by activating a ubiquitin-dependent proteolytic pathway. Nature. 2000; 405:579–583. [PubMed: 10850718]
27. Rao H, Uhlmann F, Nasmyth K, Varshavsky A. Degradation of a cohesin subunit by the N-end rule pathway is essential for chromosome stability. Nature. 2001; 410:955–959. [PubMed: 11309624]
28. Ditzel M, Wilson R, Tenev T, Zachariou A, Paul A, Deas E, Meier P. Degradation of DIAP1 by the N-end rule pathway is essential for regulating apoptosis. Nat Cell Biol. 2003; 5:467–473. [PubMed: 12692559]
29. Yoshida S, Ito M, Callis J, Nishida I, Watanabe A. A delayed leaf senescence mutant is defective in arginyl-tRNA:protein arginyltransferase, a component of the N-end rule pathway in Arabidopsis. Plant J. 2002; 32:129–137. [PubMed: 12366806]

30. Stewart AE, Arfin SM, Bradshaw RA. Protein NH2-terminal asparagine deamidase. Isolation and characterization of a new enzyme. J Biol Chem. 1994; 269:23509–23517. [PubMed: 8089117]
31. Grigoryev S, Stewart AE, Kwon YT, Arfin SM, Bradshaw RA, Jenkins NA, Copeland NG, Varshavsky A. A mouse amidase specific for N-terminal asparagine. The gene, the enzyme, and their function in the N-end rule pathway. J Biol Chem. 1996; 271:28521–28532. [PubMed: 8910481]
32. Cantor JR, Stone EM, Chantranupong L, Georgiou G. The human asparaginase-like protein 1 hASRGL1 is an Ntn hydrolase with beta-aspartyl peptidase activity. Biochemistry. 2009; 48:11026–11031. [PubMed: 19839645]
33. Schmidt TG, Skerra A. The Strep-tag system for one-step purification and high-affinity detection or capturing of proteins. Nat Protoc. 2007; 2:1528–1535. [PubMed: 17571060]
34. Gill SC, von Hippel PH. Calculation of protein extinction coefficients from amino acid sequence data. Anal Biochem. 1989; 182:319–326. [PubMed: 2610349]
35. Kane JF. Effects of rare codon clusters on high-level expression of heterologous proteins in Escherichia coli. Current Opinion in Biotechnology. 1995; 6:494–500. [PubMed: 7579660]
36. Griswold KE, Mahmood NA, Iverson BL, Georgiou G. Effects of codon usage versus putative 5′-mRNA structure on the expression of Fusarium solani cutinase in the Escherichia coli cytoplasm. Protein Expr Purif. 2003; 27:134–142. [PubMed: 12509995]
37. Salis HM, Mirsky EA, Voigt CA. Automated design of synthetic ribosome binding sites to control protein expression. Nature Biotechnology. 2009; 27:946–950.
38. Frottin F, Martinez A, Peynot P, Mitra S, Holz RC, Giglione C, Meinnel T. The proteomics of N-terminal methionine cleavage. Mol Cell Proteomics. 2006; 5:2336–2349. [PubMed: 16963780]
39. Altschul SF, Madden TL, Schaffer AA, Zhang J, Zhang Z, Miller W, Lipman DJ. Gapped BLAST and PSI-BLAST: a new generation of protein database search programs. Nucleic Acids Res. 1997; 25:3389–3402. [PubMed: 9254694]
40. Larkin MA, Blackshields G, Brown NP, Chenna R, McGettigan PA, McWilliam H, Valentin F, Wallace IM, Wilm A, Lopez R, Thompson JD, Gibson TJ, Higgins DG. Clustal W and Clustal X version 2.0. Bioinformatics. 2007; 23:2947–2948. [PubMed: 17846036]

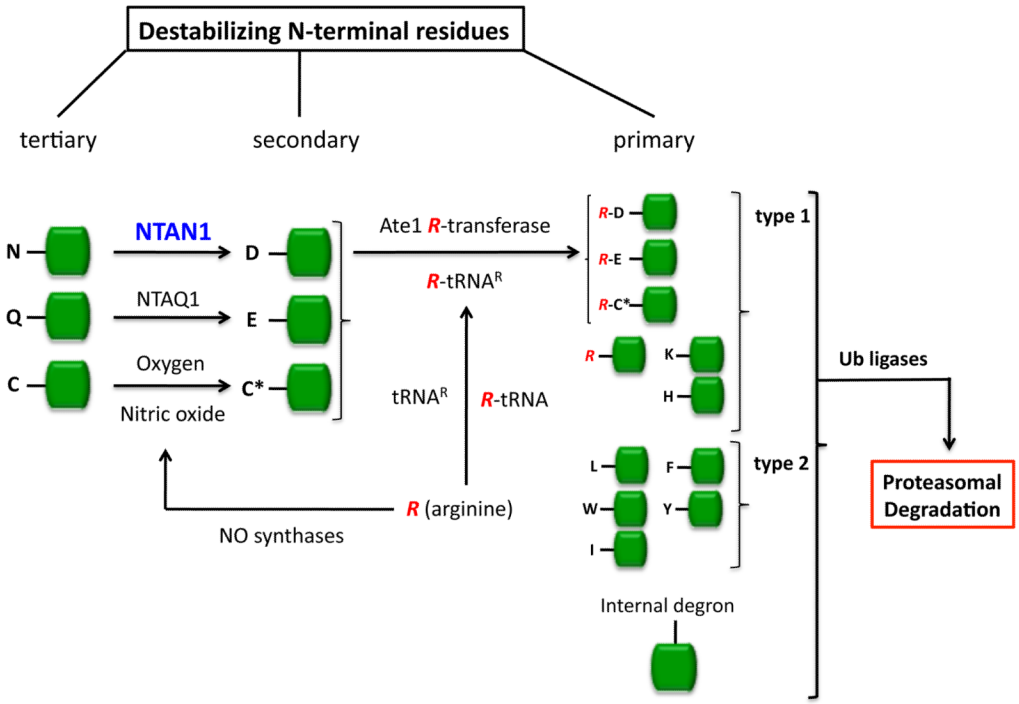


**Figure 1. The mammalian N-end rule pathway**

N-terminal residues are indicated by single-letter abbreviations. Green boxes denote the remainder of the protein substrate. C* denotes oxidized N-terminal Cys (either Cys-sulfinate or Cys-sulfonate). The Cys oxidation requires nitric oxide (NO) and oxygen or its derivatives. “Tertiary”, “secondary”, and “primary” denote mechanistically distinct subsets of destabilizing N-terminal residues (See “Introduction”). The enlarged and blue-colored “NTAN1” denotes the N-terminal asparagine amidohydrolase characterized in this study.

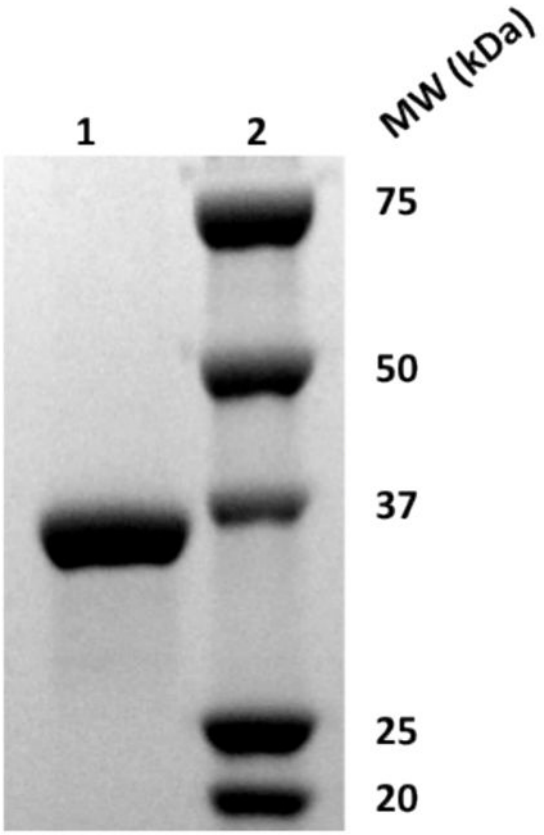


**Figure 2. SDS-PAGE analysis of hNTAN1 following tandem affinity purification**

*1*, hNTAN1 was expressed with C-terminal tandem FLAG-strepII affinity tag from pNTANFLAGSII and purified as described in detail in "Experimental Procedures". Equivalent product homogeneity was observed following analogous purification of hNTAN1 expressed from pNTAN2FLAGSII (Figure S4). *2*, M.W. marker.

(A)

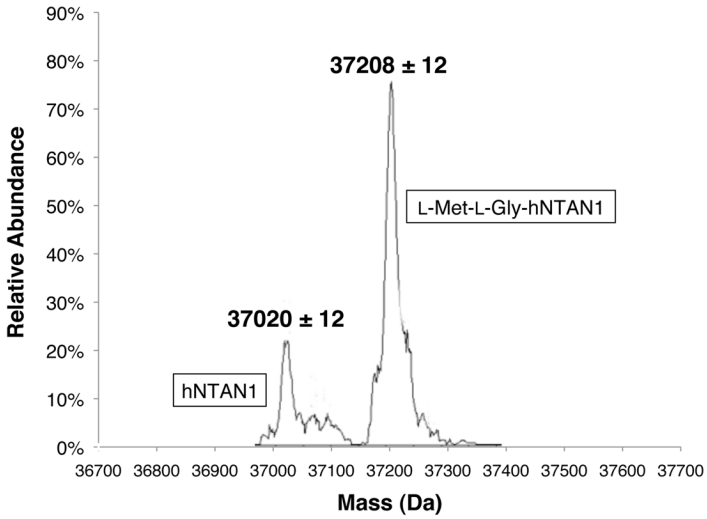


(B)

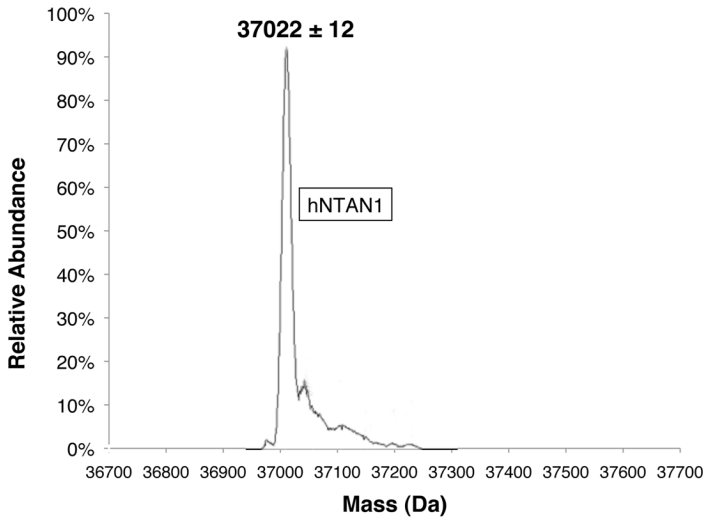


**Figure 3. Deconvoluted ESI-MS spectra of hNTAN1**

(A) hNTAN1 expressed from pNTANFLAGSII and isolated using tandem affinity purification (See "Experimental Procedures"). (B) hNTAN1 expressed from pNTAN2FLAGSII and isolated with identical tandem affinity purification protocol. Samples were analyzed in 50mM Tris-HCl, 150mM NaCl, 1mM EDTA, 0.5mM dTT, pH 7.5. Calculated masses of observed species: hNTAN1 – 37,026 Da; L-Met-L-Gly-hNTAN1 – 37, 214 Da.

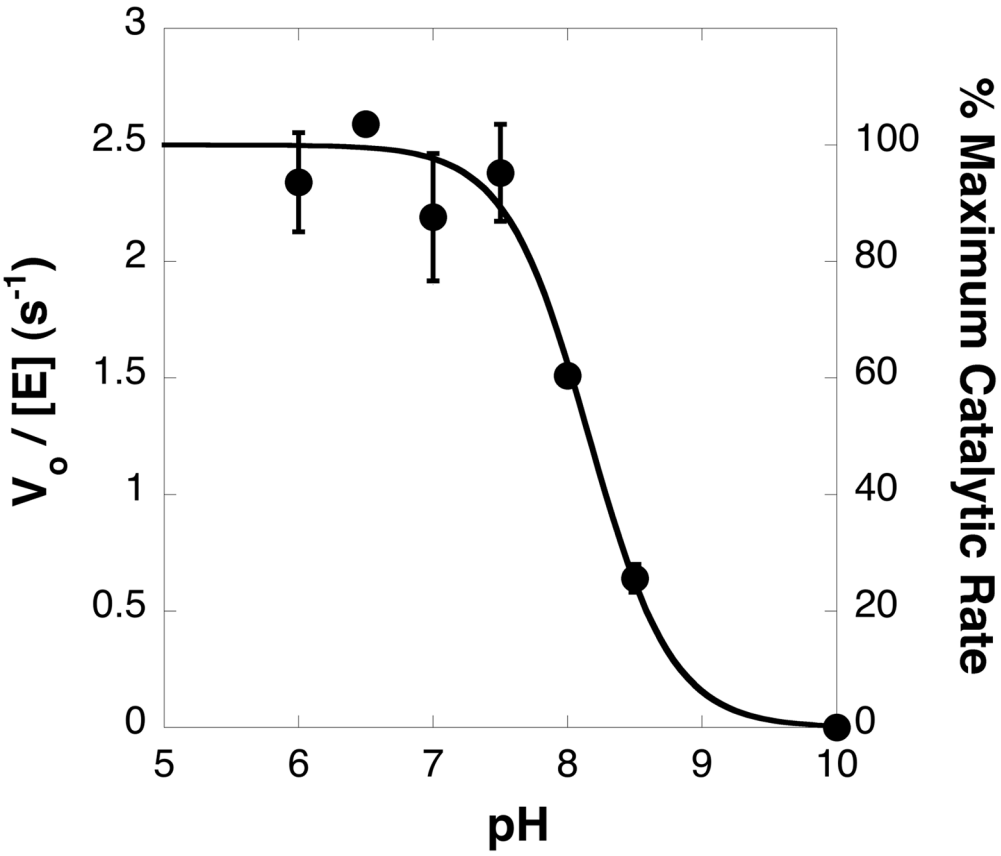


**Figure 4. Effect of pH on hNTAN1 activity**

hNTAN1 (20nM) was preincubated at the appropriate pH for 1.5min at 25°C. Reactions were initiated by the addition of the preincubated enzyme (1nM) to 25$\mu$M $N^1$-AII at 37°C in the identical preincubation buffer. After 1.5 min, reactions were quenched and then analyzed by HPLC as described in "Experimental Procedures". Activity was evaluated as the initial velocity of the reaction normalized by hNTAN1 concentration. All reactions were done in triplicate. Buffers used were: 50mM Bis-Tris, pH 6.0–6.5, 50mM Tris, pH 7.0–8.5, and 50mM CAPSO, pH 10. All buffers contained 150mM NaCl.

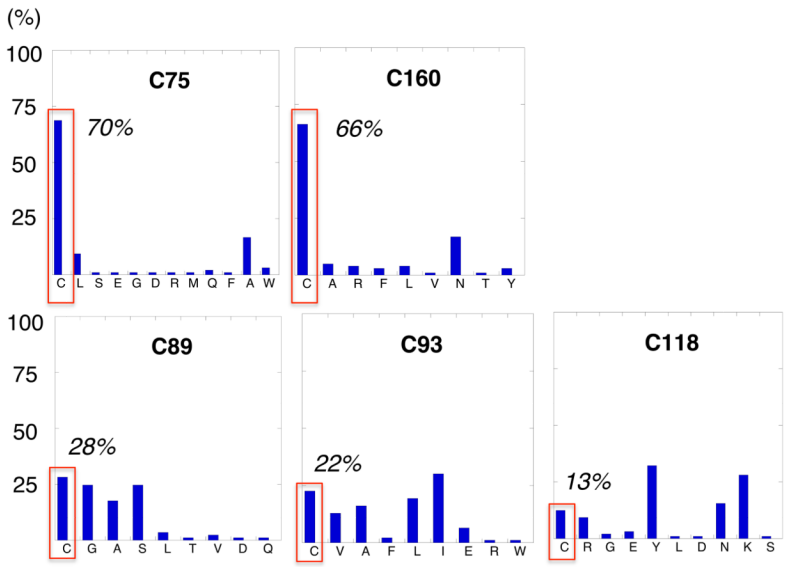


**Figure 5. Phylogenetic conservation of hNTAN1 Cys residues**

A PSI-BLAST search was carried out with the complete amino acid sequence of hNTAN1 (UniProtKB number: Q96AB6) at EMBL-EBI (http://www.ebi.ac.uk/Tools/sss/psiblast/). The "UniProt Knowledgebase" was selected as the Protein Database and the PSI-BLAST threshold was set to 10. An alignment of hNTAN1 with the PSI-BLAST results (n = 106) was generated with ClustalW2 (40) and used to evaluate the degree of conservation across each Cys residue in hNTAN1. Each plot depicts the residue identities and corresponding frequencies observed at the hNTAN1 Cys position denoted at the top of each plot. The italicized percentage value within each plot indicates the frequency of Cys (highlighted by red outline) across all sequences at the given hNTAN1 position.

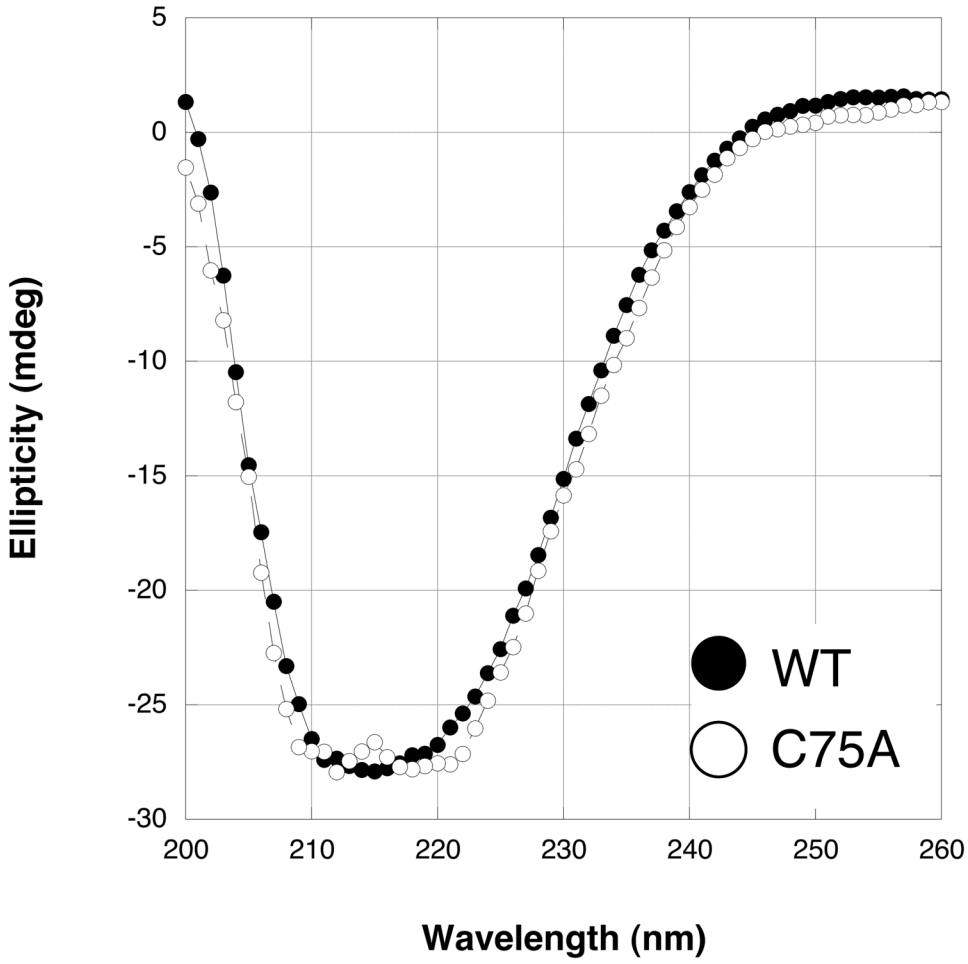


**Figure 6. Far-UV CD analyses of WT and C75A hNTAN1**

CD spectra of each sample (15$\mu$M) were recorded at 25°C in 50mM Tris-HCl, 150mM NaCl, 1mM EDTA, 0.5mM dTT, pH 7.5. The spectra shown reflect 3 accumulations per sample. WT hNTAN1 (●). hNTAN1-C75A (○). *mdeg*, millidegrees.

## Table 1
### hNTAN1 constructs and their relevant expression characteristics in BL21 (DE3)

The sequences of the sense and antisense primers used for the modified termini and RBS are found in Supplementary Table 1. The resultant amino acid sequences are shown where residues following the ellipsis are indicative of the C-terminus of the sequence. The purity of hNTAN1 was evaluated by SDS-PAGE, where band intensities were estimated by densitometry imaging (Quantity 1, BioRad).

| Plasmid | RBS | Amino Acid Sequence | hNTAN1 Purity |
|---|---|---|---|
| pHisNTAN* | AAGGAGA | MGGSSHHHHHHSSGPLLV…SGPS | 30 % |
| pNTANHis | AAGGAGA | MGPLLV…SGPSGGSSHHHHHH | 30 % |
| pR1NTANSII | AAGGAGA | MGPLLV…SPGSSAWSHPQFEK | 30 % |
| pR2NTANSII | AACAATAATAAGGAGATAAGAA | MGPLLV…SPGSSAWSHPQFEK | 70 % |
| pNTANFLAGSII | AACAATAATAAGGAGATAAGAA | MGPLLV…SPGSGGGSDYKDDDDKSAWSHPQFEK | > 98% |
| pNTAN2FLAGSII | AACAATAATAAGGAGATAAGAA | MPLLV…SPGSGGGSDYKDDDDKSAWSHPQFEK | > 98% |

* Trace activity detected for $His_6$-hNTAN1 through addition of final purified product (10$\mu$g total protein) to 1mM $N^1$-AII for 90 min at 37°C in 50mM Tris-HCl, 150mM NaCl, pH 7.5. Reactions were quenched with 12% TCA (w/v) and then evaluated by HPLC for the presence of a peak corresponding to the expected product AII. For all other plasmids, the presence of hNTAN1 activity could be detected through the addition of final purified product (10–100ng total protein) to 100$\mu$M $N^1$-AII for 1 min at 37°C in the same buffer and evaluated similarly.

## Table 2

**Summary of kinetic parameters for hydrolysis of N-terminal L-Asn angiotensin II ($N^1$-AII) by hNTAN1**

Kinetic parameters were derived from nonlinear fit of the Michaelis-Menten equation to initial rate measurements. Reactions were carried out at 37°C in 50mM Tris-HCl, 150mM NaCl, pH 7.5. The parenthetical in the enzyme column depicts whether purified hNTAN1 was expressed from pNTANFLAGSII (+ Gly2) or from pNTAN2FLAGSII (− Gly2).

| Enzyme | $K_M$ (μM) | $k_{cat}$ ($s^{-1}$) | $k_{cat}/K_M$ ($M^{-1}s^{-1}$) |
|---|---|---|---|
| hNTAN1 (+Gly2) | 31 ± 4 | 2.3 ± 0.07 | $7.4 \pm 1 \times 10^4$ |
| hNTAN1 (−Gly2) | 35 ± 3 | 6.6 ± 0.1 | $1.9 \pm 0.2 \times 10^5$ |

## Table 3
### Effects of divalent metals, EDTA, and D-desthiobiotin on hNTAN1 activity

hNTAN1 (20nM) was preincubated in 50mM Tris-HCl, 150mM NaCl, pH 7.5 at 4°C for 3 hr with either EDTA (1mM), D-desthiobiotin (3mM), or a divalent salt (1mM). Reactions were initiated by addition of the preincubated enzyme (1nM) to 100$\mu$M $N^1$-AII in 50mM Tris-HCl, 150mM NaCl, pH 7.5 at 37°C. After 4 min, reactions were quenched and then analyzed by HPLC as described in “Experimental Procedures”.

| Effector | % Activity Remaining |
|---|---|
| $MgCl_2$ | 100 |
| $CaCl_2$ | 100 |
| $CoCl_2$ | 58 ± 2.8 |
| $MnSO_4$ | 40 ±14 |
| $NiSO_4$ | 39 ± 4.2 |
| $CuCl_2$ | 0 * |
| $ZnSO_4$ | 0 |
| EDTA | 100 |
| D-desthiobiotin | 100 |

*Area of the product peak was less than or equal to that observed in an HPLC trace of $N^1$-AII only at the equivalent reaction conditions.

## Table 4

### Relative activity of hNTAN1 mutants

Reactions of hNTAN1 (40–50nM) with 100$\mu$M $N^1$-AII were carried out at 37°C in 50mM Tris-HCl, 150mM NaCl, pH 7.5. After 1 min, reactions were quenched and then analyzed by HPLC as described in "Experimental Procedures."

| Enzyme | % Relative Activity (v. WT) |
|---|---|
| WT | 100 |
| C160A | 100 |
| C75A | 0 * |
| C75S | 0 |
| C75T | 0 |

*Area of the product peak was less than or equal to that observed in an HPLC trace of $N^1$-AII only at the equivalent reaction conditions.

**Table 5**

Calculated secondary structure of WT and C75A hNTAN1 from CD spectra.

| hNTAN1 variant | % Helix | % Sheet | % Turn | % Random |
|---|---|---|---|---|
| WT | 30 | 20 | 20 | 30 |
| C75A | 30 | 20 | 20 | 30 |